

Theory of the energy-spectrum dependence of the electronic thermoelectric tunneling coefficients of a quantum dot

X. Zianni

Department of Applied Sciences, Technological Educational Institution of Chalkida, 34 400 Psachna, Greece

(Received 23 April 2008; published 29 October 2008)

The effect of the energy spectrum of a quantum dot on the electron conductance, thermopower, and thermal conductance when the dot is weakly coupled to two electron reservoirs is investigated within the sequential tunneling regime. The cases of nonequidistant and/or of degenerate energy levels spectrum are considered. Analytical formalism for the transport coefficients is derived that provides interpretation of the physical behavior of the system in the quantum regime where the discreteness of the energy spectrum of the quantum dot plays a major role in transport properties. The derived formalism refers to a general case of energy spectrum, and it can be therefore applied to real cases such as nanocrystals and molecules. It is found that the details of the energy spectrum more drastically affect the magnitude of the electron thermal conductance at low temperatures. Depending on the charging state of the quantum dot, the thermoelectric efficiency could be tuned.

DOI: [10.1103/PhysRevB.78.165327](https://doi.org/10.1103/PhysRevB.78.165327)

PACS number(s): 73.50.Lw, 73.63.Kv, 73.23.Hk

I. MOTIVATION

Transport properties have been widely studied both theoretically and experimentally in low-dimensional structures¹⁻⁴ and numerous technological applications have emerged (e.g., in electronics and optoelectronics). Considerable research activity and outcomes can also be noticed in charge transfer in nanostructures and nanodevices. Much less research has been devoted to the thermoelectric properties of these structures. The thermoelectric transport phenomena of low-dimensional and nanocomposite structures are currently attracting the research interest aiming to design structures with enhanced thermoelectric efficiency.⁵⁻⁸ The issue of efficiently converting thermal energy into electricity is the subject of active research in view of the need for energy supply from new and renewable sources that our society faces. Thermoelectric generators and cooling devices are advantageous energy converters with a wide range of applications.

A measure of the thermoelectric efficiency is the dimensionless figure of merit: $ZT = S^2 \sigma T / \kappa$, where T denotes the absolute temperature, S is the thermopower, σ is the conductivity, and κ is the thermal conductivity. In conventional materials σ and κ are related through Wiedemann-Franz law. Even the best conventional thermoelectric materials (e.g., Bi-Sb solid solutions, Bi₂Te₃-, PbTe-, and Ge-Si-based materials) have low efficiency with figure of merit not exceeding $ZT \sim 1$. Recently, novel structures such as low-dimensional nanostructures [thin films, superlattices, quantum wires, and quantum dots (QDs)] and bulk nanocomposite structures have been proposed to achieve enhancement of ZT .⁹⁻³⁰ In these structures deviations from Wiedemann-Franz law occur and it seems possible to obtain increase in the power factor ($S^2 \sigma$) and independently decrease in thermal conductivity. Reduced thermal conductivity has been found and has been attributed to electron and phonon confinement. It has been pointed out⁸ that periodicity is not necessary for enhancement of the figure of merit. At the nanoscale electrons are decoupled from phonons and their transport properties can be engineered independently.

Further understanding and theoretical models that interpret the observed behavior of the thermoelectric coefficients of low-dimensional and nanocomposite materials as well as predictive models are highly desired. The present work aims to contribute to this need. In a previous work of the author,³⁰ the electron conductance and thermal conductance of a quantum dot have been studied in the sequential tunneling regime from the quantum regime, where the discreteness of the energy spectrum is non-negligible, and to the classical regime, where Wiedemann-Franz law holds. Analytical formalism has been derived in both regimes for the conductance and the electron thermal conductance. Even earlier^{31,32} analytical formalism had been derived for the conductance and the thermopower. The analytical expressions explicitly show the dependence of the physical quantities on the characteristic parameters of the system and hence they provide direct physics insight. Moreover, they provide a useful tool to interpret experimental observations and to stimulate further experimental investigation. The analytical formulas in Refs. 30–32 hold for the special case of equidistant energy levels spectrum. This is not typical in real systems, e.g., nanocrystals, molecules, etc. Moreover, at low temperatures and for considerable quantum confinement, the details of the energy spectrum have visible effects in the transport properties, and hence the explicit relation between the measured properties and the parameters of the system is needed to interpret experimental observations. In the present work, the theoretical model of Ref. 30 is extended to the general case of energy spectrum without the assumptions of equidistant and/or nondegenerate energy levels.

The structure of the paper is as follows: in Sec. II the theoretical model is described; in Sec. III the calculated thermoelectric coefficients are presented and discussed for level-dependent energy degeneracy, g , and variable energy separation between the levels. To show the dependence of the thermoelectric coefficients on each of the above energy-spectrum characteristics, four cases are considered: (i) nondegenerate energy levels ($g=1$) and equidistant energy spectrum, (ii) nondegenerate energy levels ($g=1$) and

nonequidistant energy spectrum, (iii) degenerate energy levels and equidistant energy spectrum, and finally (iv) degenerate energy levels and nonequidistant energy spectrum. The main conclusions are drawn in Sec. IV.

II. MODEL

We consider a double barrier tunnel junction. It consists of a quantum dot that is weakly coupled to two electron reservoirs via tunnel barriers. Each reservoir is assumed to be in thermal equilibrium and there are a voltage difference V and a temperature difference ΔT between the two reservoirs. A continuum of electron states is assumed in the reservoirs that are occupied according to the Fermi-Dirac distribution,

$$f(E - E_F) = \left[1 + \exp\left(\frac{E - E_F}{k_B T}\right) \right]^{-1}, \quad (2.1)$$

where the Fermi energy, E_F , in the reservoirs is measured relative to the local conduction-band bottom.

The quantum dot is characterized by discrete energy levels $E_p (p=1, 2, \dots)$ that are measured from the bottom of the potential well. Degeneracies are to be included by multiple counting of the levels. Each level can be occupied by either one or zero electrons. It is assumed that the energy spectrum does not change by the number of electrons in the dot. The states in the dot are assumed to be weakly coupled to the states in the electrodes so that the charge of the quantum dot is well defined. We adopt the common assumption in the Coulomb-blockade problems for the electrostatic energy $U(N)$ of the dot with charge $Q = -Ne$:

$$U(N) = (Ne)^2/2C - N\varphi_{\text{ext}}, \quad (2.2)$$

where C is the effective capacitance between the dot and the reservoirs and φ_{ext} is the contribution of external charges.

The tunneling rates through the left and right barriers from level p to the left and right reservoirs are denoted by Γ_p^l and Γ_p^r , respectively. It is assumed that energy relaxation rates for the electrons are fast enough with respect to the tunneling rates so that we can characterize the state of the dot by a set of occupation numbers, one for each energy level. It is also assumed that inelastic scattering takes place exclusively in the reservoirs not in the dot. The transport through the dot can be described by rate equations.

The energy conservation condition for tunneling implies the following conditions:³¹

(i) For tunneling from an initial state $E^{i,l(r)}$ in the left (right) reservoir to a final state p in the quantum dot,

$$E^{i,l}(N) = E_p + U(N+1) - U(N) + \eta eV, \quad (2.3)$$

$$E^{i,r}(N) = E_p + U(N+1) - U(N) - (1 - \eta)eV. \quad (2.4)$$

(ii) For tunneling from an initial state p in the quantum dot to a final state in the left (right) reservoir at energy $E^{f,l(r)}$,

$$E^{f,l}(N) = E_p + U(N) - U(N-1) + \eta eV, \quad (2.5)$$

$$E^{f,r}(N) = E_p + U(N) - U(N-1) - (1 - \eta)eV, \quad (2.6)$$

where N is the number of electrons in the dot before the tunneling event and η is the fraction of the voltage V which

drops over the left barrier. The energies in the reservoirs are measured from the local conduction-band bottom.

Due to the voltage difference V and the temperature difference ΔT between the two reservoirs, electric and thermal currents pass through the dot. The stationary current I and the heat flux Q through the left barrier are, respectively, given by the following equations:

$$I = -e \sum_{p=1}^{\infty} \sum_{\{n_i\}} \Gamma_p^l P(\{n_i\}) \{ \delta_{n_p,0} f(E^{i,l}(N) - E_F) - \delta_{n_p,1} [1 - f(E^{f,l}(N) - E_F)] \}, \quad (2.7)$$

$$Q = \sum_{p=1}^{\infty} \sum_{\{n_i\}} \Gamma_p^l P(\{n_i\}) \{ \delta_{n_p,0} [E^{i,l}(N) - E_F] f(E^{i,l}(N) - E_F) - \delta_{n_p,1} [E^{f,l}(N) - E_F] [1 - f(E^{f,l}(N) - E_F)] \}, \quad (2.8)$$

where the second summation is over all possible combinations of occupation numbers $\{n_1, n_2, \dots\} \equiv \{n_i\}$ of the energy levels in the quantum dot, each with stationary probability $P(\{n_i\})$. The numbers n_i can take on only the values 0 and 1. The nonequilibrium probability distribution P is a stationary solution of a kinetic equation. This has been solved in the linear regime by Beenakker.³¹ The solution is substituted in Eqs. (2.7) and (2.8) and the linearized expressions for the electric current I and the heat flux Q are obtained as follows:

$$I = \frac{e}{k_B T} \sum_{p=1}^{\infty} \sum_{N=1}^{\infty} \frac{\Gamma_p^l \Gamma_p^r}{\Gamma_p^l + \Gamma_p^r} P_{eq}(N) F_{eq}(E_p/N) [1 - f(\varepsilon_p - E_F)] \times \left[eV - \frac{\Delta T}{T} (\varepsilon_p - E_F) \right], \quad (2.9)$$

$$Q = -\frac{1}{k_B T} \sum_{p=1}^{\infty} \sum_{N=1}^{\infty} \frac{\Gamma_p^l \Gamma_p^r}{\Gamma_p^l + \Gamma_p^r} P_{eq}(N) F_{eq}(E_p/N) [1 - f(\varepsilon_p - E_F)] \times (\varepsilon_p - E_F) \left[eV - \frac{\Delta T}{T} (\varepsilon_p - E_F) \right], \quad (2.10)$$

where $\varepsilon_p \equiv E_p + U(N) - U(N-1)$. Here, $P_{eq}(N)$ is the probability that the quantum dot contains N electrons in equilibrium and $F_{eq}(E_p/N)$ is the conditional probability in equilibrium that level p is occupied given that the quantum dot contains N electrons. The above equilibrium probabilities are, respectively, defined³¹ as

$$P_{eq}(N) = \sum_{\{n_i\}} P_{eq}(\{n_i\}) \delta_{N, \sum n_i}, \quad (2.11)$$

$$F_{eq}(E_p/N) = \frac{1}{P_{eq}(N)} \sum_{\{n_i\}} P_{eq}(\{n_i\}) \delta_{n_p,1} \delta_{N, \sum n_i}. \quad (2.12)$$

Here, $P_{eq}(\{n_i\})$ is the Gibbs distribution in the grand canonical ensemble:

$$P_{eq}(\{n_i\}) = Z^{-1} \exp \left[-\frac{1}{k_B T} \left(\sum_{i=1}^{\infty} E_i n_i + U(N) - N E_F \right) \right], \quad (2.13)$$

where $N \equiv \sum_i n_i$ and Z is the partition function:

$$Z = \sum_{\{n_i\}} \exp \left[-\frac{1}{k_B T} \left(\sum_{i=1}^{\infty} E_i n_i + U(N) - N E_F \right) \right]. \quad (2.14)$$

In the regime of linear response, the current I and the heat flux Q are related to the applied voltage difference V and the temperature difference ΔT by the equations¹

$$\begin{pmatrix} I \\ Q \end{pmatrix} = \begin{pmatrix} G & L \\ M & K \end{pmatrix} \begin{pmatrix} V \\ \Delta T \end{pmatrix}. \quad (2.15)$$

The thermoelectric coefficients are related by Onsager relation that in the absence of a magnetic field is

$$M = -LT. \quad (2.16)$$

Equation (2.15) can be re-expressed with the current I rather than the voltage V as an independent variable,

$$\begin{pmatrix} V \\ Q \end{pmatrix} = \begin{pmatrix} R & S \\ \Pi & -\kappa \end{pmatrix} \begin{pmatrix} I \\ \Delta T \end{pmatrix}. \quad (2.17)$$

The resistance R is the reciprocal of the isothermal conductance G . The thermopower S is defined as

$$S \equiv - \left. \frac{V}{\Delta T} \right|_{I=0} = -L/G. \quad (2.18)$$

The Peltier coefficient is defined as

$$\Pi \equiv \left. \frac{Q}{I} \right|_{\Delta T=0} = M/G = ST, \quad (2.19)$$

where Eq. (2.16) has been used in the second equality.

Finally, the thermal conductance is defined as

$$\kappa \equiv - \left. \frac{Q}{\Delta T} \right|_{I=0} = -K \left(1 + \frac{S^2 GT}{K} \right). \quad (2.20)$$

By comparison of the above definitions of the transport coefficients with the linearized expressions for I and Q , the following expressions are extracted for the transport coefficients:

$$G = \frac{e^2}{k_B T} \sum_{p=1}^{\infty} \sum_{N=1}^{\infty} \gamma_p P_{eq}(N) F_{eq}(E_p/N) \times \{1 - f[Ep + U(N) - U(N-1) - E_F]\}, \quad (2.21)$$

$$S = -\frac{e}{k_B T^2 G} \sum_{p=1}^{\infty} \sum_{N=1}^{\infty} \gamma_p [E_p + U(N) - U(N-1) - E_F] \times P_{eq}(N) F_{eq}(E_p/N) \{1 - f[Ep + U(N) - U(N-1) - E_F]\}, \quad (2.22)$$

$$K = -\frac{1}{k_B T^2} \sum_{p=1}^{\infty} \sum_{N=1}^{\infty} \gamma_p [E_p + U(N) - U(N-1) - E_F]^2 \times P_{eq}(N) F_{eq}(E_p/N) \{1 - f[Ep + U(N) - U(N-1) - E_F]\}, \quad (2.23)$$

where

$$\gamma_p \equiv \frac{\Gamma_p^l \Gamma_p^r}{\Gamma_p^l + \Gamma_p^r}. \quad (2.24)$$

Expressions (2.21) and (2.22) have been for the first time obtained in Refs. 25 and 37.

The above findings for the transport coefficients can be written in the following more general formalism for the transport coefficients:³⁰

$$G = L^{(0)}, \quad (2.25)$$

$$S = -\frac{1}{eT} (L^{(0)})^{-1} L^{(1)}, \quad (2.26)$$

$$K = \frac{1}{e^2 T} L^{(2)}. \quad (2.27)$$

The electron thermal conductance, κ , is given by the expression

$$\kappa = -\frac{1}{e^2 T} [L^{(2)} - L^{(1)}(L^{(0)})^{-1} L^{(1)}], \quad (2.28)$$

where

$$L^{(\alpha)} = \frac{e^2}{k_B T} \sum_{p=1}^{\infty} \sum_{N=1}^{\infty} \frac{\Gamma_p^l \Gamma_p^r}{\Gamma_p^l + \Gamma_p^r} [E_p + U(N) - U(N-1) - E_F]^{(\alpha)} \times P_{eq}(N) F_{eq}(E_p/N) \{1 - f[Ep + U(N) - U(N-1) - E_F]\}. \quad (2.29)$$

III. CALCULATED THERMOELECTRIC COEFFICIENTS

The formalism of the previous section has been used to calculate transport coefficients for quantum dots with non-equidistant energy levels and/or with degenerate energy levels. In what follows, numerical calculations of G , S , and κ for representative energy spectra are presented and they are interpreted by appropriate new theoretical formalism for the transport coefficients in the quantum regime, where the thermal energy is smaller than the separation between the energy levels of the dot.

A. Nondegenerate energy levels ($g=1$)

1. Equidistant energy spectrum

Figures 1–3 show plotted calculated transport coefficients using Eqs. (2.25)–(2.29) for representative values of the parameters in the case of energy spectrum with equidistant energy levels and for level-independent tunneling rates. Peri-

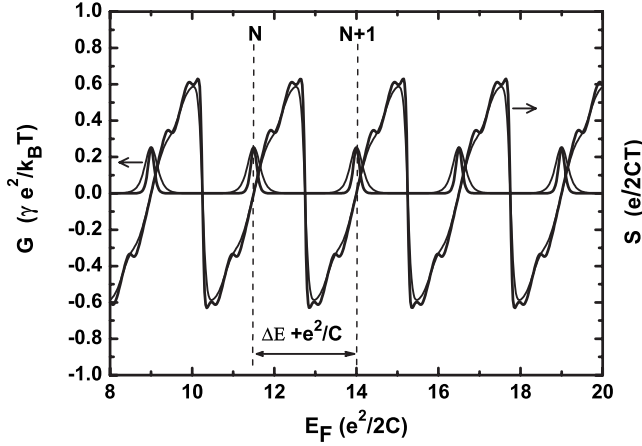


FIG. 1. Calculated conductance, G , and thermopower, S , for a series of equidistant energy levels with separation $\Delta E = 0.5e^2/2C$ and for $k_B T = 0.05e^2/2C$ (thick solid lines) and $k_B T = 0.1e^2/2C$ (thin solid lines).

odic Coulomb-blockade oscillations are exhibited. The peaks of the conductance, thermopower, and thermal conductance occur each time an extra electron enters the QD with periodicity:

$$\Delta E_F = \Delta E + e^2/C, \quad (3.1)$$

where ΔE is the constant energy level separation and the discrete energy levels are $E_p = p\Delta E$ ($p = 1, 2, \dots$). In Fig. 1, the additional sawtooth short-period oscillations of the thermopower are due to the discreteness of the energy spectrum.³²

Due to the discreteness of the energy spectrum a single charging state contributes to transport and the term with $N = N_{\min}$ gives the dominant contribution to the sums over N in Eq. (2.29), where N_{\min} is the integer that minimizes the absolute value of $\Delta(N) = E_N + U(N) - U(N-1) - E_F$. It is

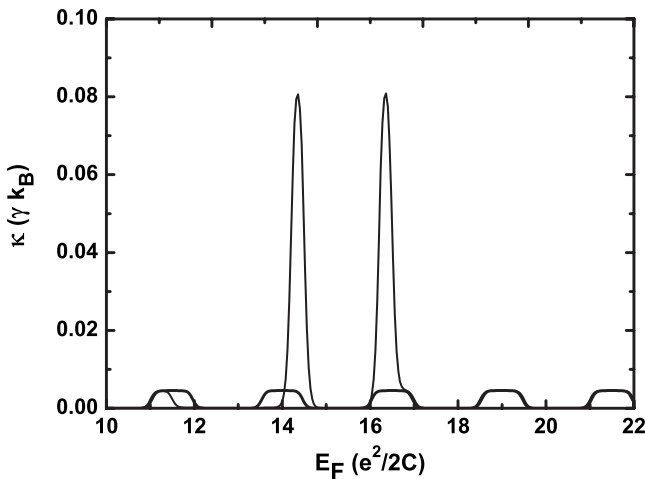


FIG. 2. Calculated thermal conductance, κ , for a series of equidistant energy levels with separation $\Delta E = 0.5e^2/2C$ (thick solid line) and for an energy spectrum with the same level separation with a single irregularity introduced (the energy of one level has been shifted by $0.2e^2/2C$) (thin solid line) for $k_B T = 0.05e^2/2C$.

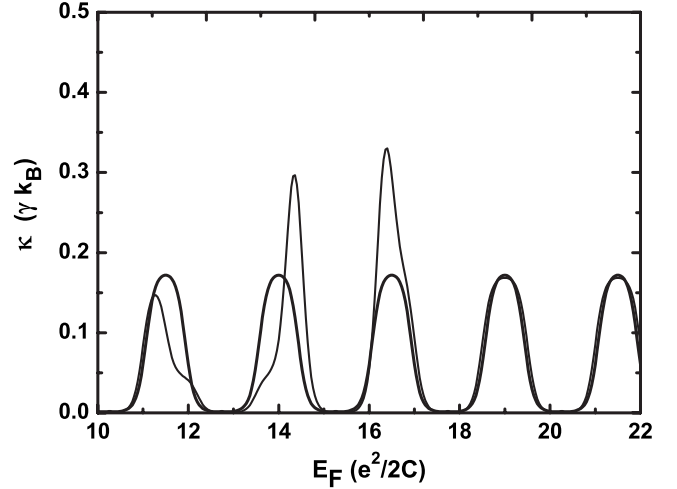


FIG. 3. As in Fig. 2, for $k_B T = 0.1e^2/2C$.

defined: $\Delta \equiv \Delta(N_{\min})$ and $\Delta_p \equiv E_p - E_{N_{\min}}$. For $\Delta < 0$, the sum over the energy levels in Eq. (2.29) extends over the integers $N_{\min}, N_{\min}+1, \dots, N_C$, where N_C is the largest integer such that $\Delta_p + \Delta < 0$. For $\Delta > 0$, the sum extends over the integers $N_{\min}, N_{\min}-1, \dots, N_C$, where N_C is the smallest integer such that $\Delta_p + \Delta > 0$. When approximate expressions are used for the distribution functions, simplified formulas are obtained for the conductance, G , and the thermopower, S ,³²

$$G = \frac{e^2}{4k_B T} \gamma \frac{1}{\cosh^2(\Delta/2k_B T)} \left[\text{Int} \left(\frac{|\Delta|}{\Delta E} \right) + 1 \right], \quad (3.2)$$

$$S = -\frac{1}{eT} \left[\Delta - \frac{\Delta E}{2} \text{Int} \left(\frac{\Delta}{\Delta E} \right) \right]. \quad (3.3)$$

The above expressions are good approximations for G and S in the sequential tunneling regime that gives the main contribution to transport near the peaks of G . Near the tails and between the gaps of G (i.e., around the peaks of S) cotunneling effects are non-negligible³³ and should also be taken into account for an accurate description of the system transport properties.

For values of E_F where the conductance is nonvanishing, i.e., away from the tails and the gaps between the peaks, the summation over p in Eq. (2.29) can be restricted to the first neighbors of $p = N_{\min}$. It is then possible to obtain simplified formulas for G , S , and κ that are good approximations in the quantum regime. The derived formalism provides good description of the electron contribution to the figure of merit ($S^2 G / \kappa$) and the power factor ($S^2 G$) when the conductance and the thermal conductance are not vanishing small.

By keeping contributions from $p = N_{\min} - 1, N_{\min}$, and $N_{\min} + 1$ in Eq. (2.29) and using the quantum limit approximations of the distribution functions given in the Appendix, the following are obtained:

$$G = \frac{e^2}{k_B T} \gamma \left[\frac{1}{4 \cosh^2(\Delta/2k_B T)} + e^{-\Delta E/k_B T} \right], \quad (3.4)$$

$$S = -\frac{1}{eT} \left\{ \Delta - (\Delta E) e^{-\Delta E/k_B T} \frac{e^{\Delta/k_B T} - 1}{e^{\Delta/k_B T} + 1} \frac{1}{[G/(e^2 \gamma/k_B T)]} \right\}, \quad (3.5)$$

$$\kappa = k_B \gamma \left(\frac{\Delta E}{k_B T} \right)^2 \frac{e^{-\Delta E/k_B T}}{1 + 4 \cosh^2(\Delta/2k_B T) e^{-\Delta E/k_B T}}, \quad (3.6)$$

where $\gamma \equiv \Gamma^l \Gamma^r / (\Gamma^l + \Gamma^r)$. It is noted that in case of considerable confinement (i.e., big ΔE compared to $k_B T$), the second term in Eq. (3.4) is negligible and can be ignored.

The above expressions explicitly give the effects of confinement and of temperature on the conductance, thermopower, and thermal conductance. When quantum confinement increases, ΔE also increases and this causes a shift in the separation between the peaks of the transport coefficients as described in Eq. (3.1). Equation (3.4) shows that the increase in quantum confinement has a negligible effect in the conductance maximum (where $\Delta=0$) because the second term is vanishing small. The increase in quantum confinement has, though, a drastic effect in the thermal conductance, and this is due to the exponential dependence on the ratio of the energy level spacing over the thermal energy, $\Delta E/k_B T$, in Eq. (3.6). Hence, in quantum regime, κ decreases nearly exponentially when the size of the QD decreases due to the increase in ΔE .

Thermal energy acts against quantum confinement. The Coulomb oscillations peaks of the transport coefficients are thermally broadened as it is shown for G and S in Fig. 1. The fine structure of the short-period oscillations of S can only be distinguished at very low temperatures. The $1/T$ dependence of S [Eqs. (3.3) and (3.5)] dominates at most temperatures. G_{\max} occurs for $\Delta=0$ [Eq. (3.4)], and it decreases linearly with increasing thermal energy. κ_{\max} increases nearly exponentially with increasing thermal energy due to the exponential term in Eq. (3.6).

2. Nonequidistant energy spectrum

Let us now consider the case of a nonequidistant energy spectrum. This case is interesting because it is typical for real systems such as nanocrystals and molecules. The separation between the level corresponding to a peak and the previous (next) one is denoted by ΔE_1 (ΔE_2). Equation (3.1) relates the separation between two neighboring energy levels (ΔE) with the separation between the corresponding Coulomb peaks (ΔE_F). Therefore, it is explained why the calculated Coulomb oscillations consist of a nonperiodic sequence of peaks for a nonequidistant energy spectrum. The following analytical formula has been found a good approximation of the conductance values that are obtained using Eqs. (2.25) and (2.29):

$$G = \frac{e^2}{k_B T} \gamma \left[\frac{1}{4 \cosh^2(\Delta/2k_B T)} + \frac{e^{-\Delta E_1/k_B T} e^{\Delta/k_B T} + e^{-\Delta E_2/k_B T}}{1 + e^{\Delta/k_B T}} \right]. \quad (3.7)$$

In case of considerable confinement, the second term in this equation is negligible and hence the height of the peaks of G is only weakly affected by the separation between the energy

levels. The values of ΔE_1 and ΔE_2 , added to the charging energy [Eq. (3.1)], determine the separation of a peak from the previous peak and from the next one, respectively.

A nonperiodic sequence of peaks has been similarly found for the thermal conductance. In this case, though, the shape and the height of the peaks are considerably dependent on the details of the energy spectrum. This effect is shown in Fig. 2, where the electron thermal conductance for an equidistant energy spectrum is plotted (thick solid line), together with that for an energy spectrum with the same energy level separation ($\Delta E=0.5e^2/2C$) and with a single irregularity introduced: one energy level shifted upwards by $0.2e^2/2C$ (thin solid line). The increased energy level separation with the previous level ($\Delta E_1=0.7e^2/2C$) causes a significant decrease in κ , whereas the decreased energy level separation with the next level ($\Delta E_2=0.3e^2/2C$) causes an increase in κ . This effect becomes less significant with increasing thermal energy as it can be seen by comparing the data in Fig. 2 with those in Fig. 3 that correspond to a higher temperature. The following analytical formula provides a good approximation of the thermal conductance in this regime:

$$\kappa/k_B \gamma = \frac{(\Delta E_1/k_B T)^2 e^{-\Delta E_1/k_B T} e^{\Delta/k_B T} + (\Delta E_2/k_B T)^2 e^{-\Delta E_2/k_B T}}{1 + e^{\Delta/k_B T}} - \frac{[(\Delta E_1/k_B T) e^{-\Delta E_1/k_B T} e^{\Delta/k_B T} - (\Delta E_2/k_B T) e^{-\Delta E_2/k_B T}]^2}{(1 + e^{\Delta/k_B T})^2 [G/(e^2 \gamma/k_B T)]}, \quad (3.8)$$

where the following has been used:

$$S = -\frac{1}{eT} \left\{ \Delta - \frac{\Delta E_1 e^{-\Delta E_1/k_B T} e^{\Delta/k_B T} - \Delta E_2 e^{-\Delta E_2/k_B T}}{e^{\Delta/k_B T} + 1} \frac{1}{[G/(e^2 \gamma/k_B T)]} \right\}. \quad (3.9)$$

B. Degenerate energy levels ($g \neq 1$)

The energy-spectrum degeneracy is reflected in the Coulomb oscillations of the transport coefficients and this has been discussed in Ref. 30 for doubly-degenerate energy levels for G and κ . Here, we discuss the case of energy spectrum with the level that contributes to charge transport being degenerate with multiplicity g . The transport coefficients have been calculated using the exact formalism of Eqs. (2.25)–(2.29). Their behavior is interpreted by the analytical expressions given below that have been found to be good approximations in the quantum regime. The notation used in the equations is as follows: each peak corresponds to charging a level of degeneracy g , and g_p and g_n are, respectively, the degeneracy of the previous and of the next level. The symbol ℓ enumerates the number of electrons in the level with degeneracy g . Functions ζ_p and ζ_n are for previous and next level, respectively, and they are defined in the Appendix.

1. Equidistant energy spectrum

Here,

$$G = \frac{e^2}{k_B T} \gamma C_{\ell g} \left[\frac{\ell(1 + e^{\Delta/k_B T})}{4 \cosh^2(\Delta/2k_B T)} + \left(\zeta_p g_p e^{\Delta/k_B T} + \zeta_n g_n \frac{\ell}{g - \ell + 1} \right) e^{-\Delta E/k_B T} \right], \quad (3.10)$$

$$\kappa = k_B \gamma \left(\frac{\Delta E}{k_B T} \right)^2 e^{-\Delta E/k_B T} C_{\ell g} \left(\zeta_p g_p e^{\Delta/k_B T} + \zeta_n g_n \frac{\ell}{g - \ell + 1} \right) \left[1 - e^{-\Delta E/k_B T} \frac{\left(\zeta_p g_p e^{\Delta/k_B T} - \zeta_n g_n \frac{\ell}{g - \ell + 1} \right)^2}{\left(\zeta_p g_p e^{\Delta/k_B T} + \zeta_n g_n \frac{\ell}{g - \ell + 1} \right) [G/(e^2 \gamma/k_B T)]} \right], \quad (3.11)$$

where the following has been used:

$$S = - \frac{1}{eT} \left\{ \Delta - (\Delta E) e^{-\Delta E/k_B T} \left(\zeta_p g_p e^{\Delta/k_B T} - \zeta_n g_n \frac{\ell}{g - \ell + 1} \right) \frac{C_{\ell g}}{[G/(e^2 \gamma/k_B T)]} \right\} \quad (3.12)$$

and

$$C_{\ell g} \equiv \frac{1}{1 + \frac{\ell}{g - \ell + 1} e^{\Delta/k_B T}}. \quad (3.13)$$

2. Nonequidistant energy spectrum

Here,

$$G = \frac{e^2 \gamma}{k_B T} C_{\ell g} \left[\frac{\ell(1 + e^{\Delta/k_B T})}{4 \cosh^2(\Delta/2k_B T)} + \left(\zeta_p g_p e^{-\Delta E_1/k_B T} e^{\Delta/k_B T} + \zeta_n g_n \frac{\ell}{g - \ell + 1} e^{-\Delta E_2/k_B T} \right) \right], \quad (3.14)$$

$$\begin{aligned} \kappa/k_B \gamma = C_{\ell g} & \left[\zeta_p g_p \left(\frac{\Delta E_1}{k_B T} \right)^2 e^{-\Delta E_1/k_B T} e^{\Delta/k_B T} \right. \\ & \left. + \zeta_n g_n \frac{\ell}{g - \ell + 1} \left(\frac{\Delta E_2}{k_B T} \right)^2 e^{-\Delta E_2/k_B T} \right] \\ & - \frac{C_{\ell g}^2}{[G/(e^2 \gamma/k_B T)]} \left[\zeta_p g_p \left(\frac{\Delta E_1}{k_B T} \right) e^{-\Delta E_1/k_B T} e^{\Delta/k_B T} \right. \\ & \left. - \zeta_n g_n \frac{\ell}{g - \ell + 1} \left(\frac{\Delta E_2}{k_B T} \right) e^{-\Delta E_2/k_B T} \right]^2, \quad (3.15) \end{aligned}$$

where the following has been used:

$$\begin{aligned} S = - \frac{1}{eT} & \left\{ \Delta - \frac{C_{\ell g}}{[G/(e^2 \gamma/k_B T)]} \right. \\ & \times \left(\zeta_p g_p \left(\frac{\Delta E_1}{k_B T} \right) e^{-\Delta E_1/k_B T} e^{\Delta/k_B T} \right. \\ & \left. \left. - \zeta_n g_n \frac{\ell}{g - \ell + 1} \left(\frac{\Delta E_2}{k_B T} \right) e^{-\Delta E_2/k_B T} \right) \right\}. \quad (3.16) \end{aligned}$$

The height of the peaks of the conductance, G , increases due to the energy degeneracy by the factor $\ell(1 + e^{\Delta/k_B T})/(1 + (\ell/g - \ell + 1)e^{\Delta/k_B T})$ as the second term of Eqs. (3.10) and (3.14) is small. The degeneracy of a single level contributes to this enhancement that is hence local: the energy level separation and the degeneracy of neighboring levels mainly affect the separation between the peaks of G and practically not their height. This is shown in Fig. 4, where calculated values of G are plotted for energy spectrum with $g=1$ for all levels except for the third level ($g=2$) and for the fourth level ($g=3$). The calculations have shown that the height of the peaks of κ increases considerably due to the energy degeneracy. In this case, the effect is less local and it depends on the degeneracy of three levels: of the actual occupied level that contributes to G , of the previous occupied level, and of the next unoccupied level. This is shown for level $p=3$ and $g=2$ in Fig. 5 and for level $p=4$ and $g=3$ in Fig. 6. In Fig. 7 the thermal conductance for energy spectrum with degenerate neighboring levels ($p=3$ and $g=2$; and $p=4$ and $g=3$) is plotted to show graphically how their effects superimpose. This behavior is numerically reproduced by Eq. (3.11).

The calculated κ in the case of energy spectrum with a nonequidistant energy level separation in addition to the degeneracy described in the previous paragraph is shown in Fig. 8 for $E_3 - E_2 = 0.3$, $E_4 - E_3 = 0.7$, and $k_B T = 0.05 e^2 / 2C$.

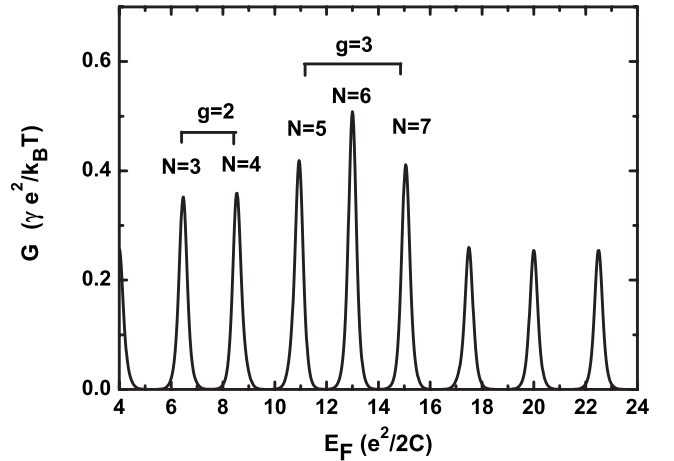


FIG. 4. Conductance, G , for equidistant energy spectrum ($\Delta E = 0.5 e^2 / 2C$) with nondegenerate levels ($g=1$) with the exception of two levels that are degenerate as shown in the figure.

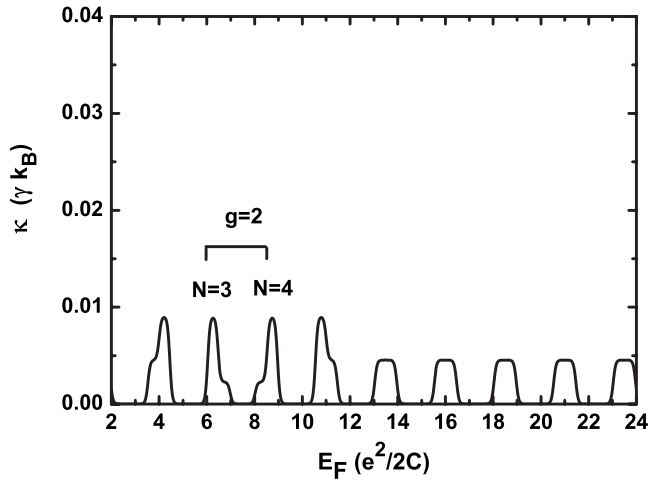


FIG. 5. Thermal conductance, κ , for equidistant energy spectrum ($\Delta E=0.5e^2/2C$) with nondegenerate levels ($g=1$) with the exception of one level with $g=2$, as explained in the figure, for $k_B T=0.05e^2/2C$.

Equation (3.15) provides a good approximation of the electron thermal conductance in this case. The calculated κ at a higher temperature $k_B T=0.1e^2/2C$ is shown in Fig. 9. It can be seen that the features of the peaks are now smoother. It can be concluded that the signature of the energy spectrum in κ is screened by the increase in κ due to increasing thermal energy.

The presented calculations have shown that in the quantum regime the details of the energy spectrum more importantly affect the magnitude of the electron thermal conductance compared with the conductance and the thermopower. Hence, when G , κ , and the power factor are not vanishing small, the figure of merit ZT is sensitive to the value of κ . Since κ is strongly energy level dependent, ZT can change considerably by changing E_F and hence the charge of the QD. It is therefore interestingly appearing a possibility for tuning the thermoelectric efficiency of a QD structure by

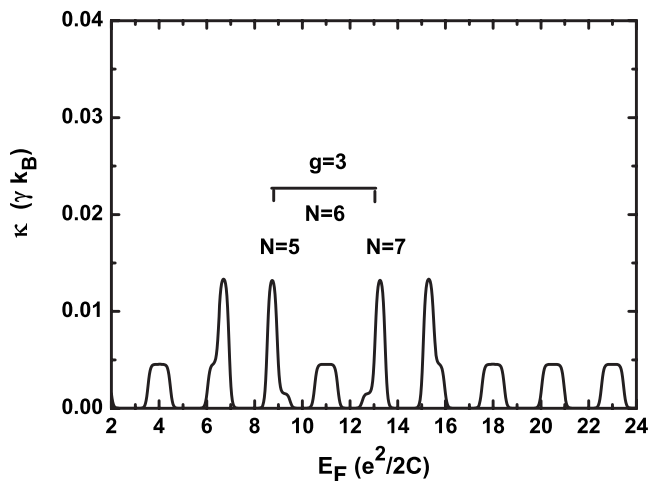


FIG. 6. Thermal conductance, κ , for equidistant energy spectrum ($\Delta E=0.5e^2/2C$) with nondegenerate levels ($g=1$) with the exception of one level with $g=3$, as explained in the figure, for $k_B T=0.05e^2/2C$.

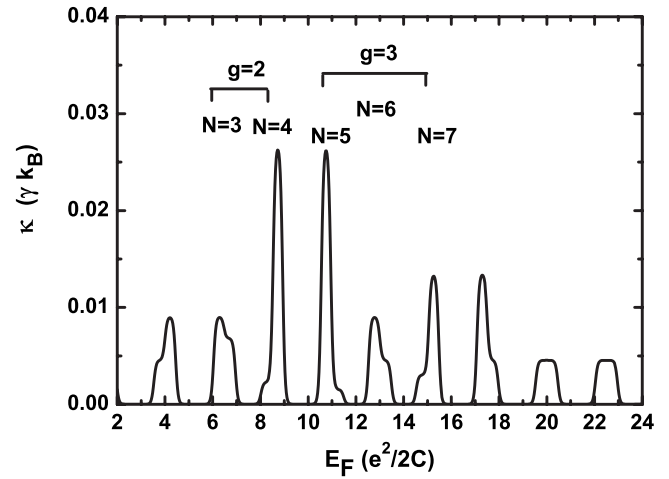


FIG. 7. Thermal conductance, κ , for equidistant energy spectrum ($\Delta E=0.5e^2/2C$) with nondegenerate levels ($g=1$) except two levels with $g=2$ and $g=3$, respectively, as explained in the figure, for $k_B T=0.05e^2/2C$.

changing its charging state. It is however left to be investigated how this behavior is modified by phonon effects.

Effects of the energy spectrum of a QD on the thermoelectric coefficients could be observable in a single-electron transistor (SET) configuration at low temperatures so that the thermal energy, $k_B T$, remains lower than the separation of the energy levels of the dot. Hence, the theory developed here can be applied to interpret experimental data on the thermoelectric coefficients and the efficiency of a SET, where the confinement region is a QD with discrete energy spectrum. Such experimental data are not yet available. There is though currently research interest and noticeable progress in this topic and this is discussed in the following part of this section.

In conventional transistors, such as a field-effect or single-electron transistor, the electric current or voltage is controlled by a gate. More recently, a different kind of working

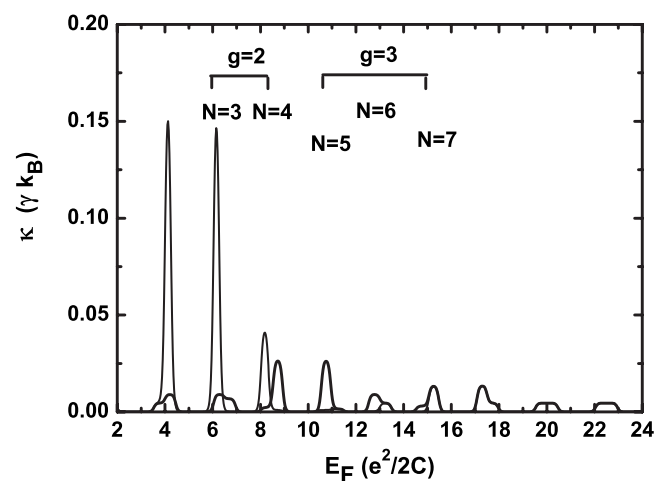


FIG. 8. Thermal conductance, κ , for equidistant energy spectrum as in Fig. 7 (thick solid line) and for nonequidistant energy spectrum as described in main text (thin solid line), for $k_B T=0.05e^2/2C$.

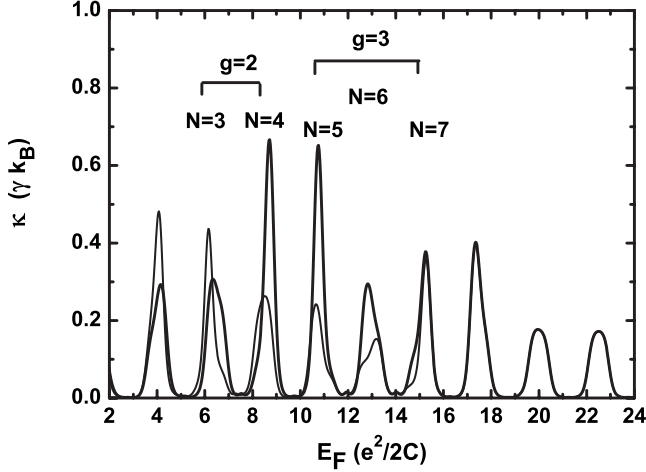


FIG. 9. As in Fig. 8, for $k_B T = 0.1 e^2/2C$.

principle was demonstrated in mesoscopic structures: the electron transport can be controlled by manipulating the quasiparticle temperature, i.e., the energy distribution of charge carriers. The realization of a heat transistor has been reported recently.³⁴ In the heat transistor under suitable bias conditions, Coulomb blockade allows the modulation of both the electric current and the heat flux. The structure investigated is a superconductor/normal-metal/superconductor (SNS) system with two insulating barriers (I) defining a superconductor/insulator/normal-metal/insulator/superconductor (SINIS) tunnel structure. The experimental findings are successfully explained through a model that associates the thermal current with single-electron tunneling. It has been proved that a normal-metal/insulator/superconductor (NIS) probe can be used as a sensitive thermometer even in the presence of charging effects, provided that the charge number distribution on the normal metal is carefully modeled. A measurement scheme for an experimental realization of a metallic single-electron transistor has been proposed³⁵ to observe the influence of Coulomb interaction on the thermoelectric transport coefficients.

The metal-based structures provide a framework for the investigation of the interplay between charging effects and heat transport at mesoscopic scale, where the size of the metallic active region is such that the discreteness of the energy spectrum can be ignored even at very low temperatures. This is not the case in semiconductor-based structures. The large magnitude difference of the Fermi wave vector between metals and semiconductors allows us to observe quantum effects in semiconductor structures much bigger than those of metal. Moreover, semiconductor-based structures offer some more advantages in comparison to metals.³⁶ A heat transistor based on a single semiconductor dot would be an ideal system to investigate experimentally the effect of the energy spectrum on the thermoelectric coefficients and the thermoelectric efficiency. Thermoelectric measurements on single dots require subtle experiments and novel techniques. Recently, a technique for measuring the temperature gradient of an electron gas across a QD has been proposed.³⁷ This method requires that the energy levels of the dot be spaced several $k_B T$ from one another. Tunneling spectroscopy

of a Ge QD in single-hole transistors with self-aligned electrodes has been reported elsewhere.³⁸ Due to self-aligned electrodes, the atomlike characteristics of a Ge QD could be observed from the tunneling current and the coupling strengths between the orbital energies of the QD and the source/drain electrodes could be revealed from the Coulomb oscillatory current spectra. Phonon effects are expected to play marginal role in interpreting these experiments since the measurements have to be kept in the quantum regime, i.e., at low temperatures so that the energy levels of the semiconductor dot are not screened by thermal energy. Hence, it seems that experimental data on the thermoelectric properties of a SET based on a semiconductor QD are to be expected soon and the theory presented here could be helpful in interpreting them.

IV. CONCLUSION

Theory of the energy-spectrum dependence of the electron thermoelectric tunneling coefficients of a QD has been developed. The presented analysis applies at low temperatures and for considerable confinement where the discreteness of the energy spectrum dominates in the behavior of the tunneling transport coefficients. The cases of nonequidistant energy spectrum and degenerate energy levels have been considered. Analytical formalism that accounts for these cases has been derived. This formalism explicitly interprets the physics of thermoelectric transport coefficients due to electrons and can be applied to real systems. To proceed with the theoretical investigation, the developed theory needs to be further expanded to include phonon effects in the thermoelectric transport coefficients at the nanoscale. As the effect of electron confinement is being explicitly and fully taken into account in the presented theoretical model, the effects of phonon energy spectrum and confinement can be unambiguously investigated.

APPENDIX: DISTRIBUTION FUNCTIONS IN THE QUANTUM REGIME

In the quantum regime, the energy level separation, ΔE , is considerable compared with the thermal energy, $k_B T$, and the distribution functions [Eqs. (2.1), (2.11), and (2.12)] can be approximated by simplified analytical expressions. Such expressions are given in Ref 30 for nondegenerate ($g=1$) and doubly-degenerate ($g=2$) levels. Here, expressions for the general case of g -degenerate levels are presented.

The following notation is used: g denotes the degeneracy of the level $p=N_{\min}$ and the symbol ℓ enumerates the number of electrons in the level of degeneracy g . It has been found that the distribution functions can be approximated by the following expressions:

$$P_{eq}(N_{\min}) \approx \frac{\begin{bmatrix} \ell \\ g \end{bmatrix} e^{-\Delta/k_B T}}{\begin{bmatrix} \ell - 1 \\ g \end{bmatrix} + \begin{bmatrix} \ell \\ g \end{bmatrix} e^{-\Delta/k_B T}} = \frac{1}{1 + \frac{\ell}{g - \ell + 1} e^{\Delta/k_B T}}, \quad (\text{A1})$$

$$F_{eq}(E_p/N_{\min}) \approx \begin{cases} 1 & \text{for } p < N_{\min} - \ell + 1 \\ \frac{\ell}{g} & \text{for } p \text{ within the multiplicity } g, \\ \frac{\ell}{g - \ell + 1} e^{-\Delta_p/k_B T} & \text{for } p > N_{\min} - \ell + g \end{cases} \quad (\text{A2})$$

$$1 - f(\Delta_p + \Delta) = \frac{e^{(\Delta_p + \Delta)/k_B T}}{1 + e^{(\Delta_p + \Delta)/k_B T}} \approx \begin{cases} e^{(\Delta_p + \Delta)/k_B T} & \text{for } p < N_{\min} - \ell + 1 \\ \frac{e^{\Delta/k_B T}}{1 + e^{\Delta/k_B T}} & \text{for } p \text{ within the multiplicity } g. \\ 1 & \text{for } p > N_{\min} - \ell + g \end{cases} \quad (\text{A3})$$

In Eq. (A3) the second equality holds in the quantum regime for $\Delta E \ll k_B T$. Nevertheless, it has been found that as ΔE increases and becomes of the order of $k_B T$, better agreement can be obtained by keeping the exact expression of the first equality when calculating the transport coefficients. To take care of this, in the analytical expressions of the main text the functions ζ have been introduced and they are defined as follows:

(i) For $p < N_{\min} - \ell + 1$:

$$\zeta_p = \begin{cases} 1 & \text{for } \Delta E \ll k_B T \\ \frac{1}{1 + e^{(\Delta_p + \Delta)/k_B T}} & \text{elsewhere} \end{cases} \quad (\text{A4})$$

(ii) For $p > N_{\min} - \ell + g$:

$$\zeta_n = \begin{cases} 1 & \text{for } \Delta E \ll k_B T \\ \frac{e^{(\Delta_p + \Delta)/k_B T}}{1 + e^{(\Delta_p + \Delta)/k_B T}} & \text{elsewhere} \end{cases} \quad (\text{A5})$$

- ¹P. N. Butcher, in *Crystalline Semiconducting Materials and Devices*, edited by P. N. Butcher, N. H. March, and M. P. Tosi (Plenum, New York, 1986).
- ²C. W. J. Beenakker and H. van Houten, *Solid State Phys.* **44**, 1 (1991).
- ³S. Datta, *Electronic Transport in Mesoscopic Systems* (Cambridge University Press, Cambridge, 1995).
- ⁴D. K. Ferry and S. M. Goodnick, *Transport in Nanostructures* (Cambridge University Press, Cambridge, 1997).
- ⁵K. Koumoto, I. Terasaki, and R. Funahashi, *MRS Bull.* **31**, 206 (2006).
- ⁶H. Boettner, G. C. Chen, and R. Venkatasubramanian, *MRS Bull.* **31**, 211 (2006).
- ⁷J. P. Heremans, *Acta Phys. Pol. A* **108**, 609 (2005).
- ⁸M. Dresselhaus, G. Chen, M. Y. Tang, R. Yang, H. Lee, D. Wang, Z. Ren, J. Fleurial, and P. Gogna, *Adv. Mater. (Weinheim, Ger.)* **19**, 1043 (2007).
- ⁹A. Khitun, K. L. Wang, and G. Chen, *Nanotechnology* **11**, 327 (2000).
- ¹⁰A. V. Andreev and K. A. Matveev, *Phys. Rev. Lett.* **86**, 280 (2001).
- ¹¹B. Lenoir, A. Dauscher, P. Poinas, H. Scherrer, and L. Vikhor, *Appl. Therm. Eng.* **23**, 1407 (2003).
- ¹²H. Beyer, J. Nurnus, H. Böttner, A. Lambrecht, T. Roch, and G. Bauer, *Appl. Phys. Lett.* **80**, 1216 (2002).
- ¹³A. A. Balandin and O. Lazarenkova, *Appl. Phys. Lett.* **82**, 415 (2003).
- ¹⁴J. L. Liu, A. Khitun, K. L. Wang, W. L. Liu, G. Chen, Q. H. Xie, and S. G. Thomas, *Phys. Rev. B* **67**, 165333 (2003).
- ¹⁵J. P. Small, K. M. Perez, and P. Kim, *Phys. Rev. Lett.* **91**, 256801 (2003).
- ¹⁶K. Wojciechowski and J. Oblakowski, *Solid State Ionics* **157**, 341 (2003).
- ¹⁷D. Vashaee and A. Shakouri, *Phys. Rev. Lett.* **92**, 106103 (2004).
- ¹⁸R. Yang and G. Chen, *Phys. Rev. B* **69**, 195316 (2004).
- ¹⁹M. C. Llaguno, J. E. Fischer, A. T. Johnson, and J. Hone, *Nano Lett.* **4**, 45 (2004).
- ²⁰T. C. Harman, M. P. Walsh, B. E. Laforge, and G. W. Turner, *J. Electron. Mater.* **34**, L19 (2005).
- ²¹A. Balandin, *J. Nanosci. Nanotechnol.* **5**, 1015 (2005).
- ²²V. Sajfert, J. P. Setrajcic, S. Jacimovski, and B. Tosic, *Physica E (Amsterdam)* **25**, 479 (2005).
- ²³Y. Bao, W. L. Liu, M. Shamsa, K. Alim, A. A. Balandin, and J. L. Liu, *J. Electrochem. Soc.* **152**, G432 (2005).
- ²⁴T. Kihara, T. Harada, and N. Koshida, *Jpn. J. Appl. Phys., Part 1* **44**, 4084 (2005).
- ²⁵M. Shamsa, W. Liu, A. A. Balandin, and J. Liu, *Appl. Phys. Lett.* **87**, 202105 (2005).
- ²⁶E. I. Rogacheva, S. G. Lubchenko, and M. S. Dresselhaus, *Thin Solid Films* **476**, 391 (2005).
- ²⁷E. I. Rogacheva, *J. Phys. Chem. Solids* **69**, 259 (2008).
- ²⁸D. Ebling, A. Jacquot, M. Jägler, H. Böttner, U. Kühn, and L. Kirste, *Phys. Status Solidi (RRL)* **1**, 238 (2007).
- ²⁹X. Zianni, *Physica E (Amsterdam)* **38**, 106 (2007).
- ³⁰X. Zianni, *Phys. Rev. B* **75**, 045344 (2007).
- ³¹C. W. J. Beenakker, *Phys. Rev. B* **44**, 1646 (1991).
- ³²C. W. J. Beenakker and A. A. M. Staring, *Phys. Rev. B* **46**, 9667 (1992).
- ³³M. Turek and K. A. Matveev, *Phys. Rev. B* **65**, 115332 (2002).
- ³⁴O. P. Saira, M. Meschke, F. Giazotto, A. M. Savin, M. Mtnen, and J. P. Pekola, *Phys. Rev. Lett.* **99**, 027203 (2007).
- ³⁵B. Kubala, J. König, and J. Pekola, *Phys. Rev. Lett.* **100**, 066801 (2008).
- ³⁶F. Giazotto, T. T. Heikkilä, A. Luukanen, A. M. Savin, and J. P. Pekola, *Rev. Mod. Phys.* **78**, 217 (2006).
- ³⁷E. A. Hoffmann, N. Nakpathomkun, A. I. Persson, H. A. Nilsson, L. Samuelson, and H. Linke, *Physica E (Amsterdam)* **40**, 1605 (2008).
- ³⁸G.-L. Chen, D. M. T. Kuo, W.-T. Lai, and P.-W. Li, *Nanotechnology* **18**, 475402 (2007).